TEMPERATURE DEPENDENCE OF KEY PERFORMANCE INDICATORS FOR AQUEOUS ELECTROCHEMICAL CAPACITORS CONTAINING NANOSTRUCTURED BIRNESSITE MANGANESE DIOXIDE

Alexander J. Roberts and Robert C.T. Slade

Chemical Sciences, University of Surrey, Guildford GU2 7XH, United Kingdom

ABSTRACT

Birnessite has been made in a number of morphologies through variation of reaction conditions in a simple templated hydrothermal synthesis. After processing into electrodes and testing in hybrid supercapacitor cells, good cyclability and a range of specific capacitances were observed. The most promising material, a birnessite nanotube, was extensively electrochemically tested at elevated temperatures. An increase in specific capacitance from around 250 to 450 F g^{-1} was observed as the temperature was raised from 30 to 80 ºC. There was a drop in specific capacitance with cycling at elevated temperatures and inferences have been drawn regarding the effects of both cycling and time spent at elevated temperatures.

Keywords: supercapacitor, MnO_2, elevated temperature, nanostructured

INTRODUCTION

A great deal of focused research on clean energy technologies for both grid power applications and an alternative to the internal combustion engine is under way worldwide, prompted by concerns of global warming and environmental sustainability. The majority of these renewable technologies do not offer security of supply and require effective energy storage. Current battery and fuel cell technologies (also seen as the only viable alternatives to the internal combustion engine), do not offer the high power densities necessary to be used on their own. Furthermore, rapid charging and discharging of such devices is likely to significantly decrease their lifetime. Electrochemical supercapacitors are attracting much attention for use both alone and in conjunction with batteries and fuel cells, as they are known to enhance the lifetime of the system by virtue of their high power densities and rapid charge-discharge characteristics [1-4].

The energy storage characteristics of supercapacitors are dependent on the physiochemical characteristics of both the electrode materials and electrolyte [1, 4-8], with the energy stored through separation of charge via accumulation at the electrode surfaces (electrical double layer capacitance [EDLC]) [9] and also through faradaic redox processes at the electrodes (pseudocapacitance) [10]. Typical commercial supercapacitors consist of carbon or ruthenium(IV) oxide (RuO_2) electrodes and an electrolyte with the highest specific capacitances being reported for hydrated RuO_2-based systems (>700 F g^{-1}), also showing good cycling ability but with problems of high cost and toxicity [10-13]. Of the metal oxides under investigation as an alternative, the most promising to date is manganese dioxide (MnO_2) with in device specific capacitances over 450 F g^{-1} and high natural abundance, low toxicity, low cost, and low environmental impact. A further advantage of MnO_2 is the range of phases and morphologies that can be attained through tailoring the manufacturing process [14-18]. Current attempts at improving performance usually center on maximizing specific surface areas and pore volumes and tailoring pore size distributions. It has been shown, however, that some birnessite MnO_2 materials exhibit high specific capacitance despite relatively low specific surface areas [19]. This is believed to be a result of the small thickness of the birnessite platelets allowing access to almost all of the MnO_2 by the electrolyte, effectively meaning that close to 100% of the material can be considered as close to the surface.

In this study, birnessite has been made in a variety of morphologies through a simple templated hydrothermal route and tested in hybrid supercapacitor cells with a neutral aqueous electrolyte. The most promising of the materials has been subject to extensive electrochemical testing at elevated temperatures in order to assess the effect on key performance indicators such as specific capacitance, current leakage, and cycle lifetime, seen by the authors as essential for future application in automobile applications.

EXPERIMENTAL

Materials Synthesis

Potassium permanganate ($KMnO_4$) (0.0949 mol) was added to potassium hydroxide (KOH)(aq) (0.5988 mol, 180 cm^3) and stirred for 30 minutes. Dodecylamine (0.0170 mol) was added and stirred for a further 30 minutes before being transferred to a Parr Hastelloy autoclave and heating to between 120 and 150 ºC for between 1 and 3 days with constant stirring (the resultant solids after washing and template removal are designated by reaction temperature and time, e.g., 1201D corresponds to 120 ºC for 1 day). After allowing the reaction to slowly cool to room temperature, the resulting solid was collected by centrifuge and washed several times with deionized water until the pH of washings corresponded to that of the starting water. The solid was then washed several times in ethanol, until all dodecylamine had been removed, checked by CHN analysis, before drying at 80 ºC overnight.

Electrodes for electrochemical characterization were prepared by mixing the material above with polyvinylidene fluoride (PVDF) and graphite in the ratio 85:5:10 in acetone with stirring for several hours to obtain a homogenous ink. The volume of the ink was reduced by heating to 85 ºC before spraying onto pre-weighed stainless steel current collectors and drying at room temperature. Carbon electrodes were prepared by the same method with MnO_2 substituted by Darco G60 carbon (Aldrich).

Assembly of Supercapacitor Cells

One MnO_2 and one carbon electrode were assembled in a hybrid arrangement separated by a glass fiber filter paper pre-soaked in $(NH_4)_2SO_4$ (aq., 2 mol dm^{-3}) electrolyte in custom test cells and were assembled to a constant torque of 2 N m^{-1}.

Characterization Techniques

Powder X-ray diffraction (XRD) profiles were measured on a PANalytical X'Pert Pro PW3179 diffractometer using CuKα radiation and an X'Celerator detector. Nitrogen sorption was carried out at 77 K on samples previously outgassed at 150 ºC for 24 hours in a Micromeritics Flowprep 060 unit. The samples were then transferred to a Micromeritics V Surface Area and Pore Size Analyzer for analysis. Samples for electron microscopy were suspended in ethanol ultrasonically for 15 minutes before being deposited on Holey carbon discs and were analyzed using a Hitatchi HD-2300A Scanning Transmission Electron Microscope (STEM) at 200 kilovolts (kV). Galvanostatic cycling of the assembled test cells was carried out between 0 and 1.35 volts over 1000 cycles at various discharge currents on a Solatron 1480 Multistat with a 1255B Frequency Response Analyzer.

RESULTS AND DISCUSSION

Powder XRD profiles of all materials synthesized between 120 and 140 ºC were of the same form, examples of which are given in Figure 1. All of the peaks observed could be indexed to potassium birnessite (ICPDF No. 00-052-0556). As both the temperature and reaction time were increased, the degree of crystallinity and/or long-range order was seen to increase, evident by an increase in relative intensity and sharpness of the peaks.

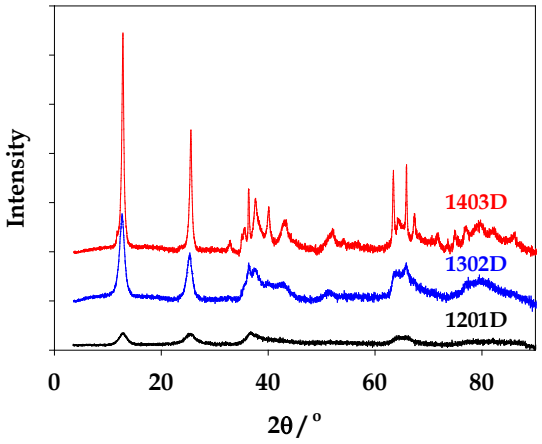

Fig. 1. Powder XRD profiles of 1201D, 1302D, and 1403D materials.

The profile observed in 1501D was of the same form, but for both 1502D and 1503D additional peaks were observed (Figure 2), becoming more prominent as the reaction time was increased. These additional peaks could be matched to the manganite phase manganese oxyhydroxide (ICPDF No. 01-074-1842). Manganite formation has been reported during attempts to synthesize birnessite nanotubes [20] and has been previously observed under these conditions

using hexadecylamine template, with the resulting electrodes showing a lesser specific capacitance than would be expected due to the presence of Mn(III) [21].

Nitrogen sorption at 77 K of all materials showed isotherms that could be classified as a combination of types I and IV as classified by BDDT [22] with a rapid uptake of nitrogen at low relative pressures (suggesting the presence of micropores) and no plateau observed at high relative pressures. Hysteresis was observed upon desorption (suggesting the presence of mesopores) with hysteresis loops classified as H3 and or H2 according to IUPAC classifications [23], suggesting a complex network of interconnected slit-shaped pores.

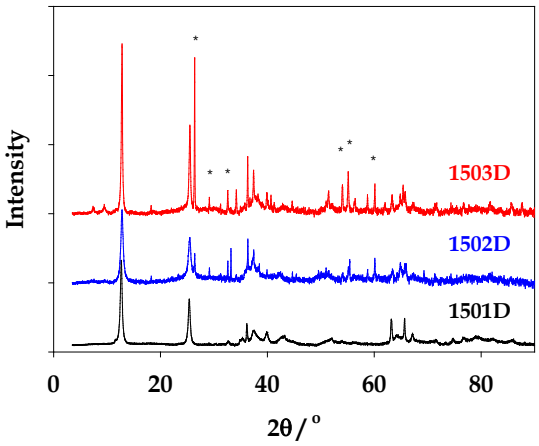

Fig. 2. Powder XRD profiles of 1501D, 1502D, and 1503D materials. Peaks corresponding to manganite are indicated by an asterisk (*).

BET analysis of the sorption isotherms showed the specific surface areas to vary depending on reaction conditions between 45 and 128 m^2 g^{-1} with total pore volumes, V_p, calculated from the nitrogen adsorption at p/p^o = 0.99 ranging from 0.17 to 0.72 cm^3 g^{-1} (see Table 1). With the exception of 1302D, the specific surface areas were seen to increase as reaction time increased but decrease with increasing reaction temperature. Although no clear trend was observed with respect to reaction conditions and total pore volume, both the 120 and 140 ºC materials showed an increase with longer reaction times.

Pore size distributions calculated using Density Functional Theory showed their relationship with reaction conditions to be complex, dependent on both reaction time and temperature. At least two peaks were observed in each case, with those of the materials formed at 150 ºC being at a higher pore diameter than those formed at lower temperatures.

Table 1. Specific surface area (SBET) and total pore volume (VP) of materials (as determined by BET and BJH analysis respectively) of the N2 isotherms at 77 K.

	S_{BET} / m^2 g^{-1}	V_p / cm^3 g^{-1}
1201D	108	0.17
1202D	116	0.35
1203D	128	0.60
1301D	46	0.09
1302D	100	0.22
1303D	48	0.09
1401D	84	0.17
1402D	84	0.19
1403D	87	0.59
1501D	45	0.72
1502D	48	0.22
1503D	64	0.33

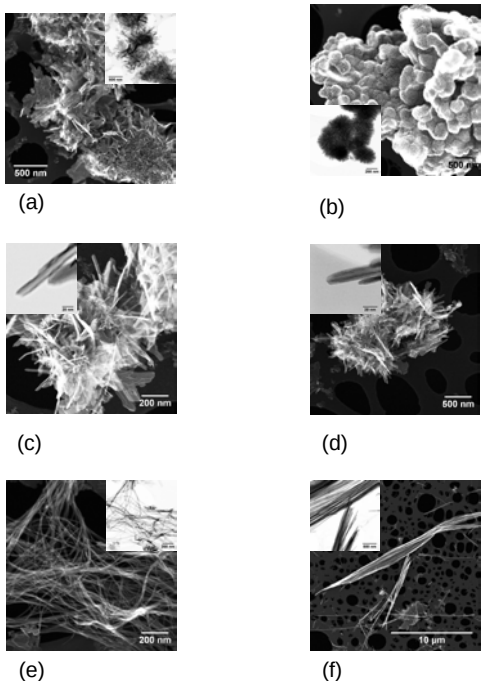

Fig. 3. Electron microscopy studies: SEM images of (a) 1201D, (b) 1202D, (c) 1203D, (d) 1303D, (e) 1403D, and (f) 1503D. TEM images are shown as insets with scale bars representing 500 nm in (a) and (f), 200 nm in (b) and (e) and 20 nm in (c) and (d).

Scanning and transmission electron micrographs (TEMs) of a number of the materials are shown in Figure 3. By inspection of the micrographs, it is apparent that small variations in reaction conditions have a major effect on particle morphology.

All of the materials were evaluated as potential supercapacitor electrodes through galvanostatic charge-discharge cycling in test cells in hybrid configuration with a carbon-based second electrode and $(NH_4)_2SO_4$ (aq., 2 mol dm^{-3}) electrolyte. The materials were cycled between 0 and 1.35 volts at a current density of 1 A g^{-1}. The expected sawtooth charge-discharge profile was observed in all materials with the charge and discharge portions being symmetrical. Excellent cyclability was observed with coulombic efficiencies between 99 and 100% being observed after the first few cycles. The specific capacitance observed after 1000 cycles, ranging between 40 and 105 F g^{-1}, are shown in Figure 4. The materials synthesized at 120 and 150 ºC showed increasing specific capacitance with increasing reaction time, following the same trend as specific surface area for the materials. Interestingly, no correlation was found between the total pore volumes and specific capacitance of these materials (the total pore volume in the 150 ºC materials decrease with reaction time, whereas those of the 120 ºC materials increase). No correlation could be inferred between the specific capacitance observed for the materials synthesized at 130 or 140 ºC and any of the properties measured in this work. This is likely due to the complex interaction (both positive and negative) of a number of contributing factors in the systems, with matters made even more complex by the presence of manganite in some of the higher temperature materials (as observed in XRD).

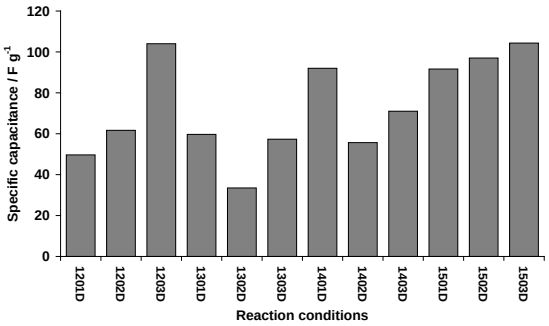

Fig. 4. Specific capacitance of materials as obtained from galvanostatic cycling at a discharge current density of 1 A g^{-1}.

One material was chosen for further electro-chemical evaluation at a variety of temperatures. Criteria for material selection for this further study were cost, ease of processing, and preliminary specific capacitance. 1203D, 1401D, and all of the 150 ºC materials exhibited comparable high specific capacitance, all of which were suitable for further study on this basis alone. Of the materials showing a high specific capacitance, 1203D produced a stable ink that sprayed with ease when making test electrodes, with the other materials requiring tighter rheological control and much effort to obtain the same electrodes of the same quality. Given these facts and consideration that higher temperature during reaction would be likely to increase overall final cost, the material chosen for further study at varied temperatures was 1203D.

The effect of temperature on specific capacitance of 120D at various discharge current densities is shown in Figure 5. As the current density was increased the specific capacitance was seen to decrease at all temperatures. This was a result of kinetically controlled diffusion in the system. As the temperature was increased, a large increase in specific capacitance of almost 100% was observed at low current density; this became less significant at higher current densities. Little difference was observed in specific capacitance between 30 and 70 ºC in measurements at higher current densities, with a significant increase being observed as the temperature was increased between 70 and 80 ºC. This increase in specific capacitance can be explained by the fact that the kinetics of diffusion in the system will be greatly increased at higher temperatures, allowing a more rapid diffusion of NH_4^+ ions into the electrode pore structure. It is believed that between 30 and 70 ºC the increase in temperature is not sufficient to increase the specific capacitance at higher discharge current densities, but at 80 ºC the diffusion is such that a large gain in specific capacitance is observed even at 10 A g^{-1} current density.

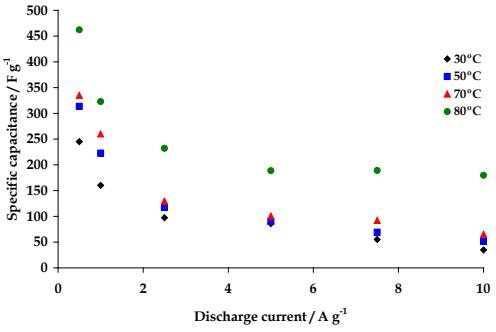

Fig. 5. Variation in specific capacitance of 1203D with discharge current density as a function of temperature.

The effect of elevated temperature on the lifetime of supercapacitors was also investigated (Figure 6). Galvanostatic cycling at a discharge current density of 2.5 A g^{-1} at 30 ºC showed an initial increase in specific capacitance over the first few cycles, with little variation observed thereafter. At 50 ºC, after an initial increase in specific capacitance over the first few cycles, little variation was observed up to 700 cycles, after which a slow fade in specific capacitance began. At 70 ºC the initial increase in specific capacitance was followed after 200 cycles by a gradual decline up to 700 cycles, after which the specific capacitance showed little variation. At 80 ºC an initial rapid increase in specific capacitance over the first 200 cycles was followed by a rapid loss over the next 200 cycles, becoming more gradual thereafter but still decreasing at 1000 cycles. After 1000 cycles the specific capacitance at 80 ºC was lower than that at 50 ºC and comparable to that at 30 ºC. At 70 ºC the loss of specific capacitance had resulted in a final value lower than that at 30 ºC.

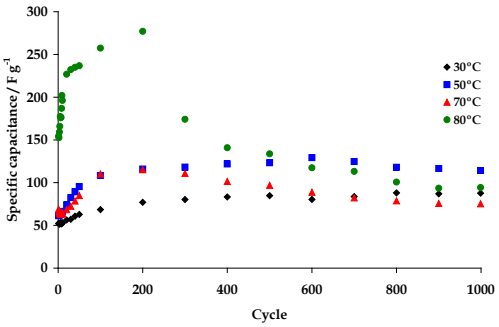

Fig. 6. Effect of cycling at various temperatures on specific capacitance calculated from galvanostatic data.

The drop in specific capacitance during cycling at 80 ºC appeared greater than might be anticipated. Given that galvanostatic testing experiments such as this involve variable time, depending upon the specific capacitance, the devices exhibiting higher initial performance spend longer at elevated temperature than those at 30 and 50 ºC. As a result of this, and in an attempt to further understand the large drop in cycling performance at 80 ºC, the effect of time at elevated temperatures was also investigated. As can be seen in Figure 7, the specific capacitance at 30 ºC showed an initial increase over the first 3 days of storage, returning to its initial value after 28 days. At 50 and 70 ºC, a less significant increase was observed initially, followed by a rapid loss over the first day before stabilizing with little change observed after 10 days at temperature. When stored at 80 ºC, a large relative increase in specific capacitance was again observed with a rapid and prolonged loss over the next 7 days or so. The specific capacitance was seen to continue to drop, approaching 0 after 15 days. These results suggest that the number of cycles performed at elevated temperatures may have a lesser effect on the lifetime of a supercapacitor device such as this than the amount of time the device spends at elevated temperatures. This was further emphasized when the cells were cycled at elevated temperatures at a charge rate of 10 A g^{-1}. At the higher discharge current densities, the time at temperature still increased as the temperature increased (due to the increase in specific capacitance) but the difference in times at temperature was considerably less. In this case the specific capacitance after 1000 cycles was seen to increase with increasing temperature, showing little effect of the differences in time that the various cells had been under test.

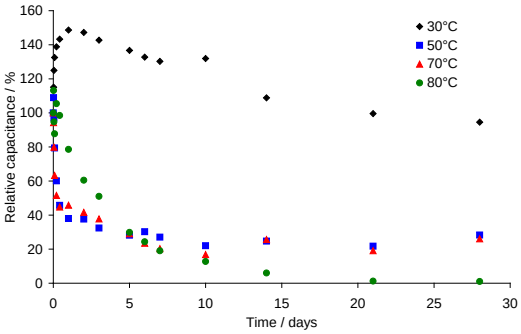

Fig. 7. Effect of storage time at elevated temperatures on specific capacitance. Relative capacitance is calculated based upon time = 0 specific capacitance.

CONCLUSIONS

Birnessite MnO_2 has been successfully made in a number of different morpholgies through variation of reaction conditions in a simple hydrothermal synthesis. Phase pure materials were obtained up to 140 ºC, with the manganite manganese oxyhydroxide phase also being formed at higher temperatures. A range of specific surface areas and pore volumes was observed, with the specific surface area generally increasing with increasing reaction time. An initial assessment of specific capacitance of the materials in hybrid supercapacitor cells with aqueous neutral electrolyte showed a variation between 40 and 105 F g^{-1}. The 1203D material was chosen for study of key performance indicators at elevated temperatures. As the temperature was increased from 30 to 80 ºC, the specific capacitance was seen to increase by nearly 100%. Galvanostatic cycling at 2.5 A g^{-1} showed a loss of capacitance, becoming more significant as the

temperature was increased; at 70 and 80 ºC, values after 1000 cycles were lower than those at the 30 and 50 ºC respectively. Furthermore, through investigation of the effect of elevated temperature storage of the devices, it was shown that the number of cycles performed under such conditions is not the sole factor determining the lifetime of such supercapacitors.

REFERENCES

[1] B.E. Conway, *Electrochemical Supercapacitors*, Scientific Fundamental and Technological Applications, Kluwer Academic/Plenum, New York, 1999.

[2] Q. Wang, Z. Wen, and J. Li, "A hybrid supercapacitor fabricated with a carbon nanotube cathode and a TiO2-B nanowire anode," *Advanced Functional Materials* **16**, 2009, pp. 2141- 2146.

[3] G. Lota, K. Lota, and E. Frackowiak, "Nanotubes based composites rich in nitrogen for supercapacitor application," *Electrochemistry Communications* **9** 2007, pp. 1828-1832.

[4] A. Chandra, A.J. Roberts, E. Lam How Yee, and R.C.T. Slade, "Nanostructured oxides for energy storage applications in batteries and supercapacitors," *Pure and Applied Chemistry* **81**, 2009, pp. 1489-1498.

[5] J. Chmiola, Y. Yushin, Y. Gogotsi, C. Portet, P. Simon, and P.L. Taberna, "Anomalous Increase in Carbon Capacitance at Pore Sizes Less Than 1 Nanometer," *Science* **313**, 2006, pp. 1760-1763.

[6] A.K.C. Gallegos and M.E. Rincon, "Carbon nanofiber and PEDOT-PSS bilayer systems as electrodes for symmetric and asymmetric electrochemical capacitor cells," *Journal of Power Sources* **162**, 2006, pp. 743-747.

[7] E. Frackowiak, V. Khomemko, K. Jurewicz, K. Lota, and F. Beguin, "Supercapacitors based on conducting polymer/nanotubes composites," *Journal of Power Sources* **153**, 2006, pp. 413-418.

[8] C. Merino, P. Soto, E.V. Ortego, J.M.G.D. Salazar, F. Pico, and J.M. Rojo, "Carbon nanofibres and activated carbon nanofibres as electrodes in supercapacitors," *Carbon* **43**, 2005, pp. 551-557.

[9] H.Y. Lee and J.B. Goodenough, "Supercapacitor behavior with KCl electrolyte," *Journal of Solid State Chemistry* **144**, 1999, pp. 220-223.

[10] S.C. Pang, M.A. Anderson, and T. Chapman, "Novel electrode materials for thin-film ultracapacitors: Comparison of electrochemical properties of sol-gel-derived and electrodeposited manganese dioxide," *Journal of the Electrochemical Society* **147**, 2000, pp. 444-450.

[11] J. P. Zheng and T.R. Jow, "The limitations of energy density for electrochemical capacitors," *Journal of the Electrochemical Society* **144**, 1997, pp. 2026-2031.

[12] W. Sugimoto, K. Yokoshima, Y. Murakami, and Y. Takasu, "Charge Storage Mechanism of Nanostructured Anhydrous and Hydrous Ruthenium-Based Oxides," *Electrochimica Acta* **52**, 2006, pp. 1742-1748.

[13] B.E. Conway, V. Briss, and J. Wojtowicz, "The Role and Utilization of Pseudocapacitance for Energy Storage by Supercapacitors," *Journal of Power Sources* **66**, 1997, pp. 1-14.

[14] A.J. Roberts and R.C.T. Slade, "Effect of specific surface area on capacitance in asymmetric carbon/α-MnO_2 supercapacitors," *Electrochimica Acta* **55**, 2010, pp. 7460-7469.

[15] A.J. Roberts and R.C.T. Slade, "Controlled synthesis of ε-MnO_2 and its application in hybrid supercapacitor devices," *Journal of Materials Chemistry* **20**, 2010, pp. 3221-3226.

[16] S. Komaba, N. Kumagai, and S. Chiba, "Synthesis of Layered MnO_2 by Calcination of $KMnO_4$ for Rechargeable Lithium Battery Cathode," *Electrochimica Acta* **46**, 2000, pp. 31-37.

[17] X. Wang, X. Wang, W. Huang, P.J. Sebastian, and S. Gamboa, "Sol-gel template synthesis of highly ordered MnO_2 nanowire arrays," *Journal of Power Sources* **140**, 2005, pp. 211-215.

[18] V. Subramanian, H. Zhu, and B. Wei, "Nanostructured MnO_2: Hydrothermal Synthesis and electrochemical Properties as a Supercapacitor Electrode Material," *Journal of Power Sources* **159**, 2006, pp. 361-364.

[19] T. Brousse, M. Toupin, R. Dugas, L. Athouel, O.Crosnier, and D. Belanger, "Crystalline MnO_2 as possible alternatives to amorphous compounds in electrochemical supercapacitors," *Journal of the Electrochemical Society* **153**, 2006, pp. A2171-A2180.

[20] L. Tao, C.-G. Sun, M.-L. Fan, C.-J. Huang, H.-L. Wu, Z.-S. Chao, and H.-S. Zhai, "A redox-assisted supramolecular assembly of manganese oxide nanotube," *Materials Research Bulletin* **41**, 11, 1996, pp. 2035-2040.

[21] A.J. Roberts and R.C.T. Slade, "Birnessite nanotubes for electrochemical supercapacitor electrodes," *Energy & Environmental Science* **4**, 2011, pp. 2813-2817.

[22] K.S.W. Sing, D.H. Everett, R.A.W. Haul, L Moscou, R.A. Pierotti, J. Roquerol and T. Siemieniewska, "Reporting physisorption data for gas/solid systems with special reference to the determination of surface area and porosity (Recommendations 1984)," Pure and Applied Chemistry **57**, 1985, pp. 603-619.

[23] J. Rouquerol, D. Avnir, C.W. Fairbridge, D.H. Everett, J.H. Haynes, N. Pernicone, J. D. F. Ramsay, K.S.W. Sing, and K.K. Unger, "Recommendations for the characterization of porous solids (Technical Report)," Pure and Applied Chemistry **66**, 1994, pp. 1739-1758.

BIOGRAPHICAL NOTE

Conference presenter: Bob Slade is Professor of Energy Chemistry at the University of Surrey (25 miles from London, UK) and leads a team of 20+ researchers in sustainable electrochemical generation and storage of electrical energy. He trained at the University of Oxford and has previously held posts in the UK at the Universities of York, Oxford, and Exeter. Current programs include pioneering work in alkaline membrane fuel cells, leadership of the UK consortium on biological fuel cells, strategic development of supercapacitors utilizing sustainable materials exhibiting pseudocapacitance, and a program in materials development and testing for redox flow batteries. He is the UK representative on the EuCheMS (European Association for Chemical and Molecular Sciences) working party on energy.